PEDESTRIAN INJURY MECHANISMS & CRITERIA
A COUPLED EXPERIMENTAL AND FINITE ELEMENT APPROACH

Catherine Masson
Pierre-Jean Arnoux
Christian Brunet
Laboratory of Applied Biomechanics. French National Institute for Transport and Safety Research-Faculty of Medicine of Marseille, Marseille, France
Dominique Cesari
Scientific Direction. French National Institute for Transport and Safety Research. Bron, France
Paper number 05-0335

ABSTRACT

In pedestrian injury biomechanics, knees and lower legs are highly recruited, leading to joint damage and bones failures. Safety improvements should mainly focus on knee ligaments injury minimization. To investigate the corresponding injury mechanisms and postulate on injury criteria risk, both experimental and finite element simulation approaches were performed. The lower limb behavior was first studied in lateral bending and then in lateral shearing impact tests in order to isolate injury mechanisms effects. The tests consisted in evaluating lower limb forces and kinematic through a 37kg guided impact with velocities ranged between 15 & 20kph. 35 tests were performed on isolated PMHS lower limbs. Response corridors for the time history about the mean response curve ± one standard deviation with the Maltese procedure were established. The observed damages were contact injuries (head of fibula and lateral tibial condyle fractures), ligament injuries (cruciates and collaterals ligaments according to the tests) and bone fractures (extra and diaphysis). These experimental tests were simulated using a finite element model of the lower limb (with extended impact velocities). The model response analysis (bone Von Mises stress levels, Ligaments global and local strain levels, knee rotation and shearing measurements) was performed during each step of the impact chronology. It leads to postulate on injury criteria for knee soft tissues based on the knee ultimate lateral bending (~16°) and shearing levels (~15mm). These approaches by coupling PMHS experimentation and numerical simulation ensure an accurate description of pedestrian lower limb trauma in terms of injury chronology and threshold. These results were also relevant with accidentology and clinical knowledge, especially with the evaluated potential injuries.

INTRODUCTION

Although the number of pedestrian suffering severe or fatal injuries has decreased since 1991 in EU (Kallina, 2002), pedestrian safety has become a major issue of society and is one of the most discussed topics in vehicle safety. If pedestrian sustain multisystem injuries, head and lower extremities injuries are the most frequently injured body regions. Particularly, lower limbs are highly loaded during crash situations (AIS from 2 to 6) with joints damages and bones failures (IHRA 2001, Stutts 1999). To improve understanding of the mechanisms and establishing tolerance criteria for this specific body part, coupled experimental and numerical studies were conducted.

Experimental studies were performed to represent condition of pedestrian accident focusing on the lower limb. The tests should have reflected the nature and the severity of the injuries sustained from this kind of impact. There is little data available from experimental studies measuring the response of the human knee joint in the pedestrian environment. Aekbote et al (Aekbote, 2003) reviewed the biomechanical studies conducted over the last three decades. He noted that mainly the injury mechanisms of the lower extremity were investigated. Tests were conducted in pure lateral shear loads, in pure bending moments or a combination of lateral shearing and bending of the knee (Kajzer 1990, Kajzer 1993, Grzegorz 2001). On cadavers full leg experiments, Kajzer (1990, 1993) focused on lower limb response under shearing and bending solicitation. He showed that pure shearing induces collateral tibial and anterior cruciate ligaments failure while a primarily bending mainly induces medial collateral ligament failure. More generally, three primary injury mechanisms were underlined: acceleration of the leg induced contact injuries as fracture of the femur and/or tibial shaft, shear force through the knee joint led to ACL rupture/avulsion, tibial intercondylar eminence fracture and femoral cartilage injury, and injuries due to bending moment at the knee joint are compression fracture of lateral femur condyle, tibial plateau fracture and MCL rupture.

These last years, recent studies have reported the response of the isolated knee joint to bending and shearing forces (Kerrigan, 2003). These tests aimed to investigate into the failure thresholds of the lower extremity. In bending tests, femoral and tibia ends were held. In this experimental configuration, MCL injuries were the most common. In shearing tests, damage to the ACL was the only relevant ligamentous injury. More recently, Bose (2004) performed 3-point bending tests on isolated knee joints in order to obtain a combination of shearing and bending effects, and confirmed injuries to medial collateral and anterior cruciate ligaments. It can be noted that knee injuries are not restricted to the injuries described above. Tibia fractures (especially with at the tibial eminence in contact with the intercondylar notch at impact), PCL injuries, fibula and femur fractures can also be observed. From all these studies, it appears that the main challenge for improving leg protection should focus on knee ligament damage and failure minimization.

Much of the most recent researches on pedestrian injury using PMHS has solely focused on sustained injuries. They reported in details bone and ligament injuries, proposed injury criteria and gave only typical load or accelerometric responses of the lower limb. These data are not always sufficient to assure a satisfactory validation of the model (Bhalla, 2003; Kerrigan, 2003; Bose, 2004; Ivarsson, 2004; Ivarsson, 2005). Very few presented response corridors to impact though they are useful to validate pedestrian surrogate models for biofidelity against PMHS test data. That why we decided to re-analyse the results of previous studies performed in Inrets-LBA (Kajzer, 1990, 1993) and to establish force-versus time corridors for bending and shearing tests.

In order to more accurately describe the injury mechanisms involved in such trauma situations, finite element simulations are more and more useful as they can provide data unavailable experimentally. In the literature, many finite element models have been designed to study very specific points of the leg behaviour under crash situations. Some ankle-foot models focused on the kinematics (Beaugonin, 1996; Beillas, 1999), others on material properties (Beaugonin, 1997; Tannous, 1996) and others else on an accurate description of geometry (Beillas, 1999). Knee models were also developed both for frontal impacts (Hayashi, 1996; Atkinson, 1998) and pedestrians (Yang, 1997; Schuster, 2000; Takahashi, 2003). Lastly, Bedewi (1996) included mathematical joints in order to control the kinematics of a full lower limb model. The THUMS model (Chawla, 2004) or the LLMS model (Arnoux, 2001-2004; Beillas, 2001) are advanced finite element models of the whole lower limb. This last model was based on an accurate description of all anatomical parts of the lower limb, and its validation was performed in various impact situations (isolated materials, sub-segments up to the whole model). It has been used to complete experimental results analysis by focussing on ligaments strain levels as a function of lateral shearing or flexion according to the load cases with an extended range of velocity.

EXPERIMENTAL STUDY

Material and methods

A linear impactor rig was used to perform dynamic PMHS tests, Figure 1. The cylinder had a mass of 37kg including instrumentation. The contact area was a flat piece with 50 mm Styrodur padding surface.

Impact experiments were conducted on 34 pairs of human lower limbs. The subjects are Post Mortem Human Subjects (PMHS) who have given voluntary before dying their body to the science. The cadaver specimens are from a population with considerably advanced age. Haut (Haut, 1995) reported that cadaver age is not significant predictor of impact biomechanics or injury to the human knee. All subjects were preserved at 3°C in Winkler's preparation (Winkler, 1974). These injection methods allow to keep supple the sampling and to preserve for several months the soft tissues elasticity. The joint range of physiological mobility was checked by medical team. Measurements of valgus-varus and knee laxity were performed. X-Rays radiographs of the body were taken and the osseous integrity in 2 planes (sagittal plane and frontal plane) was checked by an anatomist surgeon. The subjects chosen were with an average age of 78±8 years, average weight of 66±11kg, and average height of 161±21cm. Anthropometric details of the subjects are reported in Table 1. These values are both large as compared to the 50th percentile male dummy specifications of 1.73m in height and 74.5 kg in weight.

Table 1.
Cadaver Physical data.

	Age	Weight (kg)	Height (cm)	Limb Weight (kg)
Bending tests at 4.4m/s	76±6	70±8	166±4	14.4±1.9
Bending tests at 5.5m/s	75±11	60±5	168±7	13.2±1.4
Shearing tests at 4.2m/s	79±6	62±9	167±10	12.1±1.9
Shearing tests at 5.5m/s	79±8	71±16	162±6	12.8±2.2

The experiment consisted in lateral impacting an isolated lower limb (leg-thigh-half pelvis) stood up straight. The thigh was blocked with 2 foam-padded plates, called the "upper plate" and the "lower plate". One was placed on the external face at femoral condyle level, about 2 cm below the knee joint line. The second was placed on the internal face at pubic bone level. The foot was on a mobile plate to minimize ground friction and a mass of 40kg allowed preloading the lower limb (Figure 1).

Bending impacts were performed by loading the leg just above the ankle joint. The impactor was equipped with a foam-padded face of 50mm of Styrodur and 150mm×50mm of size. Distance between the knee joint line and impactor axis on the one hand and between the knee joint line and the lower plate on the other hand were recorded before test. The impact tests were performed at two impact velocities: 4.4m/s (MFG01-MFG06) and 5.5m/s (MFG07-MFG15).

Shearing tests were performed by loading the leg with 2 impact plates fixed on the impactor, one loading the leg at the proximal end of tibia and head of fibula named the "upper impact face", and one loading the leg just above the ankle joint and named the "lower impact face". Distance between the lower plate and the upper impact interface was chosen to be 40mm. A minimize contact injuries, two foam-padded interfaces were fixed on the plates (50mm of Styrodur). These impact tests were performed at two impact velocities: 4.2m/s (FCG06-FCG15) and 5.5m/s (FCG17-FCG26).

Instrumentation and measurement

An accelerometer (Entran EGA, 250g) and a force transducer (SEDEME 20kN) equipped the face of the impactor in bending tests. They measured the impactor acceleration and the impactor force presented Figures 2-3. The lower reaction force was given by a force transducer fixed on the lower plate (SEDEME, 20kN).

In shearing tests lower impact forces were measured with a force transducer fixed to the lower impact face and presented Figures 7-8. The upper impact face was equipped with an accelerometer (Entran EGA, 250g) and a force transducer (SEDEME 20kN). The measurements of the upper impact force were given in Figures 9-10. A force transducer equipped the lower plate and recorded the femur reaction force presented Figure 11-12.

A unit, comprising 32 measurement channels ensured the conditioning, analog-digital conversion and memorisation of signal. All the channels were sampled at 10kHz for a duration of 5 sec. The data acquisition system was triggered by a contact plate on the impactor connecting with two contacts on the knee. Data was transferred to a computer for processing. Loads were collected and filtered at 180Hz. Two high-speed cameras operating at 1000 frames per second were used to provide a visual record of the tests and to allow a cinematic analysis. The locations of all high-speed cameras were measured with respect to the impact location.

Test Matrix

A total of 35 tests were performed on knee joints from PMHS. In pure bending, all tests were performed from male subjects, six tests at 4.4m/s and nine tests at 5.5m/s. In shear loading, ten tests were carried out at 4.2m/s and ten tests at 5.5 m/s. In order to study repeatability of the test procedure, tests were performed on matched pairs of knees from the same subject.

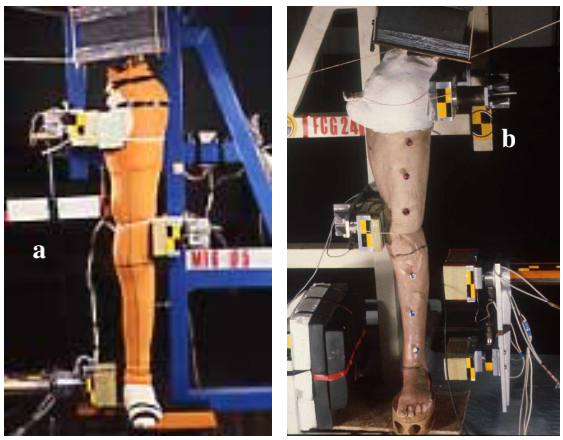

Figure 1. Setup for the bending tests (a) and for the shearing tests (b)

Corridor construction

There is not a standard methodology to construct biofidelity corridors around the cadaveric data despite the fact that the way corridors are derived is an important issue on which the biofidelity rating depends. Maltese et al (Maltese, 2002) have proposed a process for calculating corridors from test data. The first step was to scale data employing mass scaling developed by Eppinger (Eppinger, 1984) to normalize the data to a 50th percentile male subject. The scaling variable λ and the scaled test parameters with subscript s are expressed in terms of the initial parameters with subscript i in following equations.

Scaling variable $$\lambda = (75/M_i)^{1/3} \quad (1)$$

Velocity $$V_s = V_i \quad (2)$$

Acceleration $$A_s = A_i / \lambda \quad (3)$$

Time $$T_s = \lambda \times T_i \quad (4)$$

Force $$F_s = \lambda^2 F_i \quad (5)$$

Then signals were aligned by time shifting. For each sensor, one signal was chosen as characteristic response. The cumulative variance between this typical signal and each signal was calculated shifting forward then backward in time by one time step until a minimum variance (Equation 6). The calculation of cumulative variance continued until the signal was shifted in time by an amount equal to one-third of this duration in both directions

$$V_{s,k} = \sum_{t1}^{t2} (s_i - k_i)^2 \quad (6)$$

where

s_i is the magnitude of the typical signal s at t=i

k_i is the magnitude of the signal k at t=i

After time alignment, the mean response and the standard deviation was calculated at each time. To finish, mean ± one standard deviation corridors were developed. Straight lines were constructed around the mean from the defined requirements.

Experimental results

Results from bending tests

The impact force versus time corridors for the two impact velocities are presented Figures 2-3. The corridors mean shape is similar in both cases, with a linear increasing phase slightly greater at 5.5m/s. The mean peak force is 1860N at 4.4m/s and 2850N at 5.5m/s with a greater standard deviation. The duration of solicitation is comparable for both impact velocities, with a same increasing slope.

The lower reaction force corridors is plotted as a function of time for both impact velocities in Figures 4-5. The corridors show similar trends in both cases, with a first linear phase during 20ms following by a local peak. This first mean local peak is 615N at 4.4m/s and 1628N at 5.5m/s. A second peak is noticed around 50ms, slightly greater: 693 N at 4.4m/s and 1728 N at 5.5m/s.

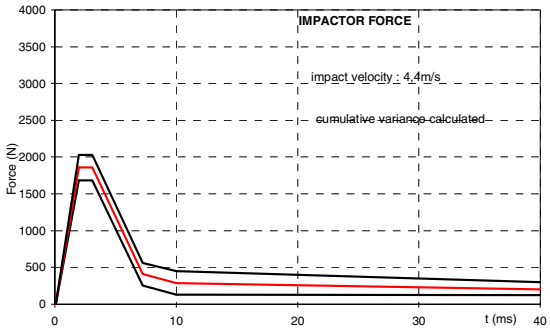

Figure 2. Impactor force corridors in bending tests at 4.4m/s.

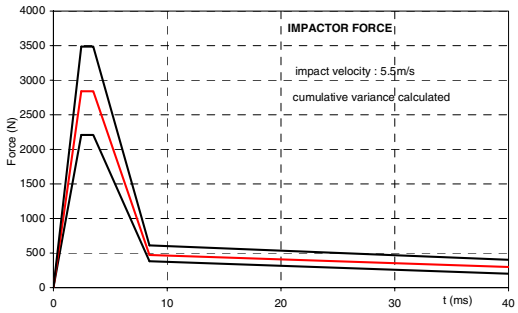

Figure 3. Impactor force corridors in bending tests at 5.5m/s.

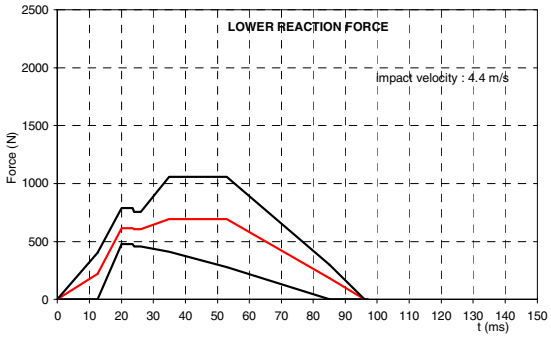

Figure 4. Lower reaction force corridors in bending tests at 4.4m/s

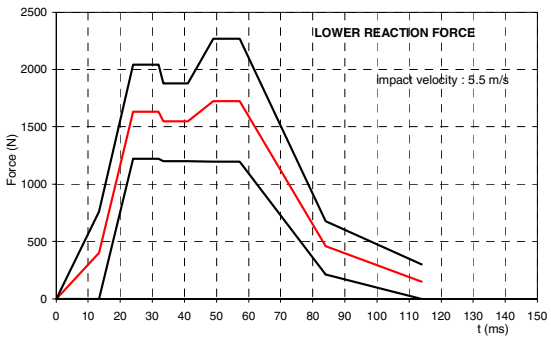

Figure 5. Lower reaction force corridors in bending tests at 5.5m/s.

A cinematic analysis was performed. The high speed images analysis provided the position at each ms. From the relative displacement of the leg against the thigh in frontal view, the lateral flexion angle of the knee was calculated (Figure 6). No significant difference appeared between 4.4m/s and 5.5m/s. It is estimated that the knee bending rate in the bending tests is approximately 1°/ms up to 13ms then is 0.5°/ms.

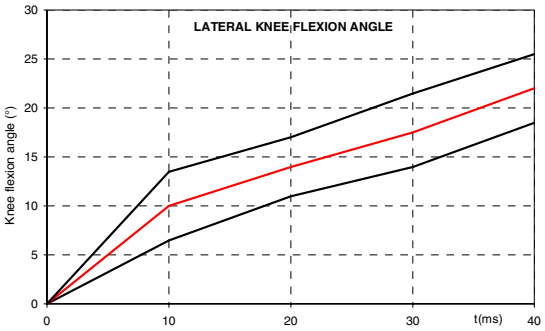

Figure 6. Knee flexion angle versus time

After testing, radiographs were taken and pre- and post-radiographs were analysed and compared. Each lower limb was then autopsied.
Tables 2 and 3 list the injuries for both series of test. Bone damage was seldom observed, only in two tests at 5.5m/s. In contrary ligament damage was observed in 70% of tests and the medial collateral ligament was always injured. The posterior cruciate ligament was never injured and damage were observed on the anterior cruciate ligament in 3 tests at 5.5m/s

Table 2.
Injuries caused in bending tests at 4.4m/s.

MFG01	MCL: avulsion at the femoral insertion
MFG02	MCL: avulsion at the femoral insertion (80%)
MFG03	MCL avulsion at the femoral insertion
MFG04	LCL : rupture (80%) in the ligament MCL : avulsion (30%) at the femoral insertion
MFG05	None
MFG06	None

Table 3.
Injuries caused in bending tests at 5.5m/s.

MFG07	LCL : partial avulsion at the femoral insertion ACL : partial avulsion at the tibial insertion
MFG08	None
MFG09	MCL: avulsion at the tibial insertion
MFG10	Tibial plate fracture
MFG11	None
MFG12	MCL: total avulsion at the femoral insertion
MFG13	MCL : avulsion at the femoral insertion Tibial plate fracture
MFG14	MCL: avulsion at the femoral insertion ACL: avulsion at the femoral insertion
MFG15	MCL: total avulsion at the femoral insertion ACL: avulsion at the femoral insertion

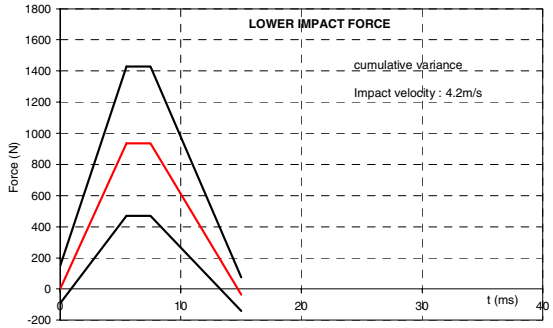

Figure 7. Lower impact force corridors in shearing tests at 4.2m/s.

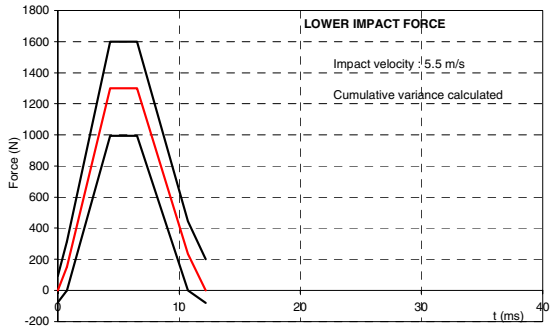

Figure 8. Lower impact force corridors in shearing tests at 5.5m/s.

Results from shearing tests

Lower impact force versus time corridors for the two impact velocities are presented Figures 7-8. The mean peak force is 935N at 4.2m/s and 1300N at 5.5m/s. The increasing phase is stiffer at 5.5m/s with a slope of 300N/ms against 170N/ms at 4.2m/s. The impact forces peak at 5.5 ms for the lower impact velocity, at 4.3ms for the second velocity and then drop to 0 by 14.8ms and 16.2ms respectively.

Figures 9-10 show upper impact force versus time corridors for both impact velocities. Three peaks are noted at 4.2m/s against only two peaks at 5.5m/s with a decreasing of the force occurring much later (60ms) than for the lowest impact velocity. If the values of the first peak differ according impact velocity (1708N and respectively 2421N), peak values on all duration are approximately the same (3000N) but appear at different times (20ms and 60ms).

Femur reaction force versus time corridors for both impact velocities are presented Figure 11-12. The corridor at 4.2m/s is very larger in time. The peak values are similar in both cases with nevertheless a slope in the increasing phase greater at 5.5m/s than at 4.2m/s (143N/ms and 306N/ms).

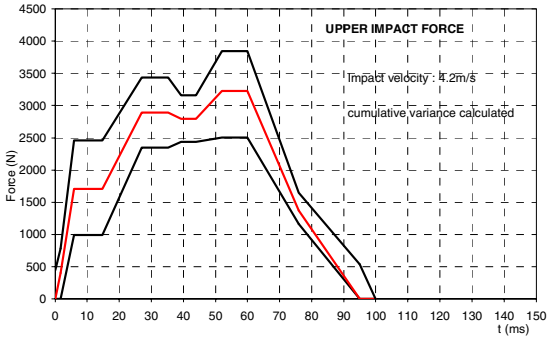

Figure 9. Upper impact force corridors in shearing tests at 4.2m/s.

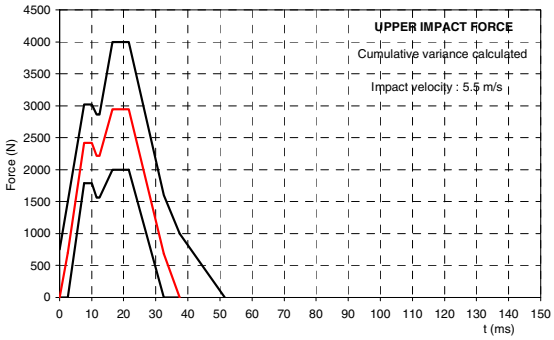

Figure 10. Upper impact force corridors in shearing tests at 5.5m/s.

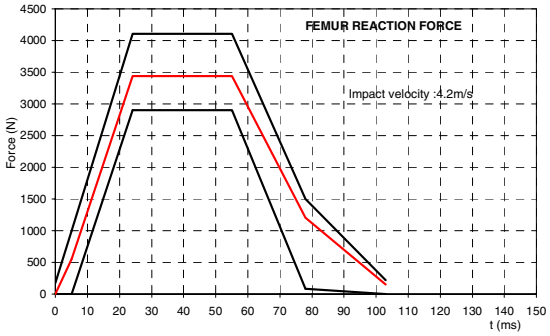

Figure 11. Femur reaction force corridors in shearing tests at 4.2m/s.

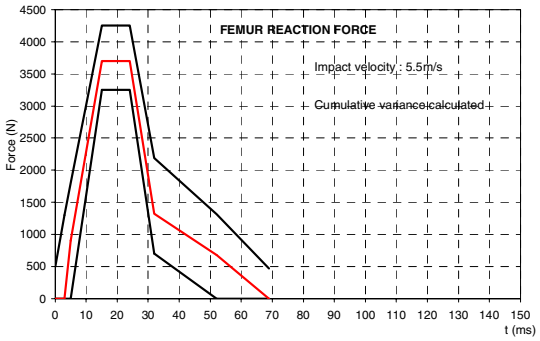

Figure 12. Femur reaction force corridors in shearing tests at 5.5m/s.

After testing, radiographs were taken and pre- and post-radiographs were analysed and compared. Each lower limb was then autopsied. Injuries are listed in Tables 4-5 and concern as well knee ligaments as lower limb bones. At 4.2m/s, concerning ligament, there were no injuries to any of the posterior cruciate ligament and only one injury to medial collateral ligament. The anterior cruciate ligament was the most often injured (in seven tests) with in six tests injury of lateral collateral ligament. Bone injuries were mainly fracture of fibula (75% of tests) and fracture of the tibial intercondylar eminence associated with femoral cartilage injury. There were no fractures to femoral diaphysis and one to tibial diaphysis. Only one knee showed no signs of fracture or any ligamentous injury. At 5.5m/s, ligament injuries were mainly anterior cruciate ligament injuries (seven tests). There were no injuries to any of the posterior cruciate ligament and few lateral ligament injuries (in 2 tests for the medial collateral and in 2 cases for the lateral collateral). Concerning bone injuries, in all cases, a fracture of the fibula was noted. We noted proportionally less tibial intercondylar eminence fracture but more tibia condyle fracture.

Table 4.
Injuries caused in shearing tests at 4.2m/s.

FCG06	None
FCG07	MCL: avulsion at the tibia insertion
FCG08	ACL avulsion at the tibia insertion, tibial intercondylar eminence crushing, femoral cartilage
FCG09	LCL : avulsion at the fibula insertion, ACL: avulsion at the tibial insertion Fracture of the lateral tibia plate Avulsion of tibial intercondylar eminence
FCG10	LCL : avulsion at the fibula insertion ACL: avulsion at the tibial insertion Avulsion of tibial intercondylar eminence
FCG11	LCL : avulsion at the fibula insertion ACL: peeling Crushing of the tibial intercondylar eminence
FCG12	LCL : avulsion at the fibula insertion ACL: peeling and partial avulsion at the tibial insertion Fracture of the fibula Crushing of the tibial intercondylar eminence
FCG13	LCL: rupture ACL: rupture at the tibial insertion Fracture of the tibia Fracture of femoral condyles
FCG14	LCL :damage ACL : avulsion (70%) at the tibial insertion Fracture of the fibula neck

Table 5.
Injuries caused in shearing tests at 5.5m/s.

FCG17	Fracture of the femoral diaphysis Fracture of the medial malleolus Fracture of the fibula (proximal end) ACL: Partial rupture (80%)
FCG18	ACL : Avulsion at the tibial insertion Fracture of the fibula diaphysis Fracture of the fibula (proximal end) Fracture of the tibia (proximal end)
FCG19	ACL : Avulsion at the tibial insertion Fracture of the fibula (proximal end) Fracture of tibial intercondylar eminence Fracture of tibial spinal tuberosity
FCG20	Crushing fracture of the medial femoral condyle Fracture of tibial intercondylar eminence Fracture of tibial spinal tuberosity Tibial cartilage injury Fracture of the fibula neck ACL: partial (80%) avulsion at the tibial insertion MCL: partial rupture
FCG21	Fracture of the femoral diaphysis Fracture of tibial intercondylar eminence Fracture of the fibula neck ACL: partial (80%) avulsion at the femoral insertion
FCG22	Fracture of the fibula (proximal end) MCL: partial rupture ACL: partial (80%) avulsion at the femoral insertion
FCG23	Fracture of the tibial diaphysis Fracture of the fibula neck
FCG24	Fracture of the fibula (proximal end) LCL: avulsion at the fibula insertion
FCG25	Fracture of tibial intercondylar eminence Fracture of the fibula diaphysis Fracture of the fibula (proximal end) ACL: avulsion at the tibial insertion
FCG26	Fracture of the fibula (proximal end) LCL : avulsion at the fibula insertion

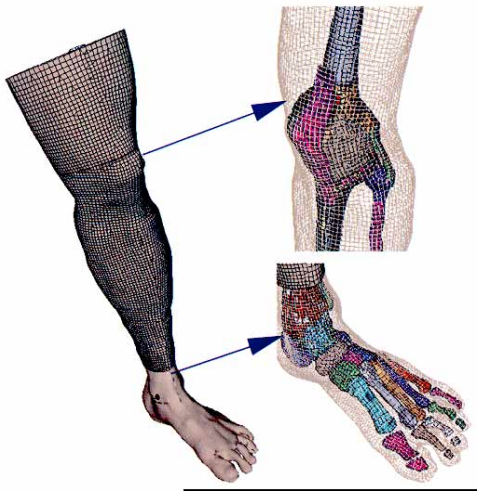

Figure 13. General overview of the Lower Limb Model for Safety (LLMS).

NUMERICAL STUDY

To complete the analysis of experimental results, a finite elements model of the lower limb (the Lower Limb Model for Safety) was used (Figure 13). As this model (validation, applications, model features) has already been presented in previously published papers (Arnoux 2001- 2004, Behr 2003- 2005, Beillas 2001), we only focus here on the use of this model to determine injury criteria assumption on the base of pedestrian related impact situations performed during experiments. In a first step model response was evaluated by comparison between simulation and reanalysis of experimental results performed in this work. Then, an analysis of model kinematics, bones Von Mises and lastly soft tissues strain levels was performed (Arnoux 2004) in order to postulate on injury assumptions

Model comparison with experiments

In Kajzer (1990) bending tests (Figure14) the upper leg was allowed to freely translate in the vertical direction, while a 22 kg dead weight was attached to the proximal femur to simulate the weight of the body. The foot was placed on a plate which allowed free translation along the direction of impact. A 40 kg impactor was used to load the distal tibia with impact velocities of 16 and 20 Kph. The model validation was achieved by comparing forces versus time recorded on the impactor face and lateral flexion by analysis of high speed video data regarding model response through new experimental corridors defined above. Results reported were relevant with experiments. Note that time amplitude was higher than experiment especially concerning unloading phase. This could be linked to soft tissue behaviour laws where physical failure was not implemented in the model.

In Kajzer (1993) shearing tests (Figure15), the leg was put in same conditions as the previous test. The impactor consists in two impacting surfaces applied simultaneously on both proximal and distal extremities of fibula and tibia. Model response was relevant with experimental corridors but do not describe complete time duration of the test. The two-stage injury mechanism experimentally identified, with the two peaks in the force time curve, was not reproduced with the LLMS model. The first injury mechanism, which occurred in 10^{th} ms after impact, is directly related to the knee impact force. It can be described as a contact injury and can induce bone fractures (head of fibula, tibia or femur). This phenomenon was relevant with Von Mises stress level recorded between tibia and fibula (Figure 16).

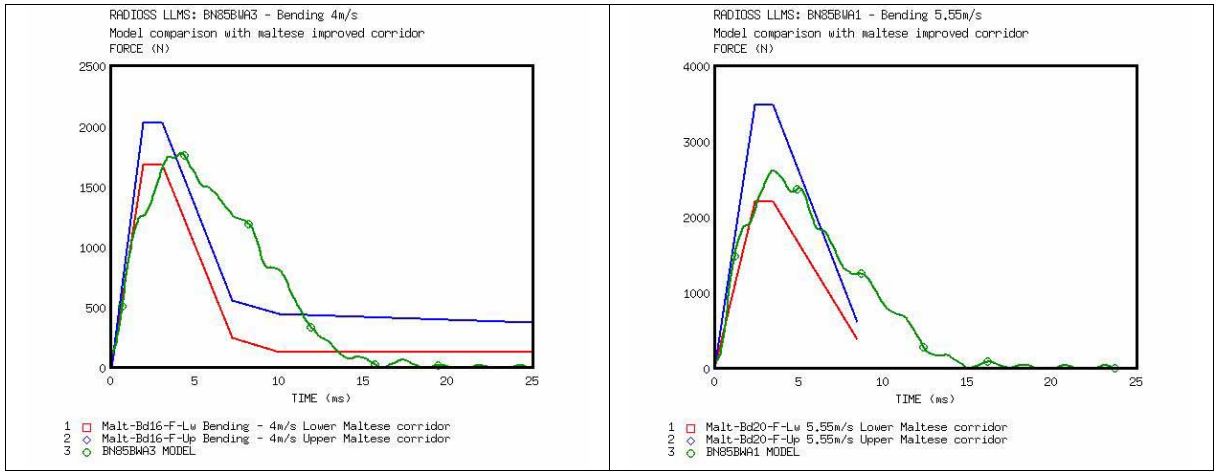

Figure 14. Comparison between simulated model and experiments of impact forces in bending tests for 16 and 20 kph impact velocities.

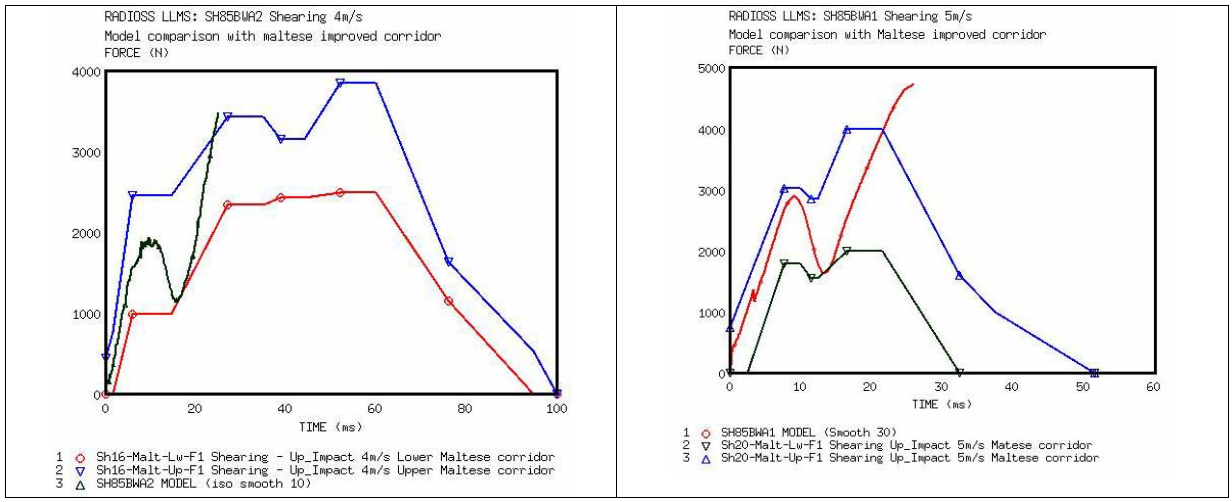

Figure 15. Comparison between simulated model and experiments of impact forces in shearing tests for 16 and 20 kph impacts velocities.

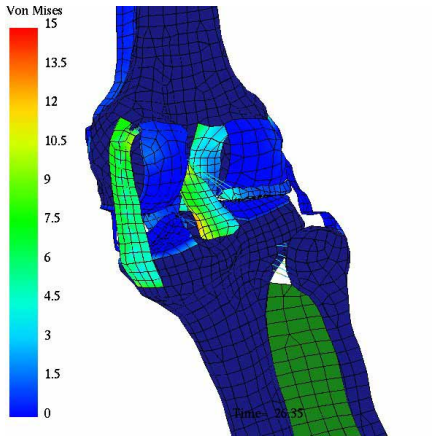

Figure 16. Illustration of Von Mises stress level in joints and recruitment level of knee ligaments.

Injury criteria evaluation

The second injury mechanism is correlated to forces transferred through the knee during acceleration of the thigh (relative shearing of tibia versus femur) which lead to soft tissues injuries. This could be linked to soft tissue behaviour laws where physical failure was not implemented in the model. Consequently, the model analysis was bounded to first part of the tests until the strain failure level on ligaments were reach. Additionally, the locations of stress concentrations predicted by the model, including the cruciate ligament insertions, the tibia eminence and the tibia fibular joint, were in agreement with the injury locations found during the autopsies (Figure 17).

Injury criteria evaluation

Taking care to the validity domain, loading cases can be extended and, from model analysis, it remains possible to compute data that is not usually recordable experimentally:
- The stress level and distribution in bones provide an estimation of damage on bone structures when stress reaches the Yield stress values.
- The kinematics was recorded to check the correct relative movements between the corresponding bones or soft tissues through knee torsion, lateral bending and frontal bending in the different planes and for each test. Therefore, the lateral relative displacement between the tibial eminence and the intercondylar notch was calculated to accurately identify knee lateral shearing at the joint level.
- Damage properties of soft tissues can be described in terms of ultimate strain levels in soft tissue structures (Arnoux 2000, Subit 2004). The results led to consider ligament failure with a strain criterion. Ultimate strain levels were calculated for the four knee ligaments and used in this study to identify potential failure. Note that literature gives various values for ultimate strain (Table 6) obtained in different experimental conditions (loading, preconditioning, conservation method…). In the present study, the ultimate values used to postulate on damage were assumed to be 28% for lateral ligaments, and 22% for cruciate ligaments. For each of the four knee ligaments, strain sensors were inserted in the model. These sensors consist in a series of springs along the main fiber axis. For the cruciate and lateral ligaments, it was also possible to compute the global strain level, the average strain level as well as the curve of maximum strain recorded at various levels in the ligament. A first step in the investigation knee joint injury criteria was to focus on previous experiments with extended impact velocities which are 2 m/s, 4 m/s, 5.55 m/s, 7 m/s and 10 m/s.

Table 6.
Overview of ultimate strain levels recorded for knee ligaments.

Author	Collateral tibial	Collateral medial	Posterior cruciate	Anterior cruciate
Viidick (1973)	30%	40%	60%	60%
Kennedy (1976)			24 (±6) %	
Marinozzi (1982)			20 (±5) %	
Prietto (1992)			28 (±9) %	
Race (1994)			18 (±5)	
Arnoux (2000)	24-38%	22-38%	15-23%	18-24%
Kerrigan (2003)	7-10%	11-20%		

For both impact situations, the Von Mises stress levels on bones were located on the proximal tibial metaphysis and distal femoral metaphysis (Figure 17). With impact velocity upper than 7m/s Von Mises stress reach 120-130MPa which is closed to failure. Bone failure on shell element was obtained by deleting elements once ultimate strain is reach. Note that model stress distribution and failure location were relevant with experiments (with lower impact velocities).

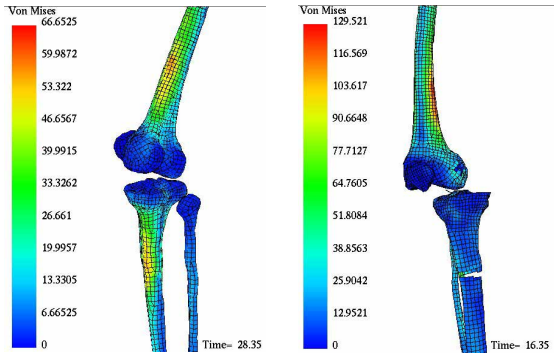

Figure 17. Typical Von Mises stress on bones for bending and shearing impact.

Model kinematics in bending tests exhibit typical lateral rotation between the tibia and the femur which seems to be correlated with velocity. The frontal rotation is stable whereas torsion effect seems to be important and correlated to the impact velocity (Figures 18 and 19). Variations of angles reach values ranging from 2° to 8°, depending on the impact velocity.

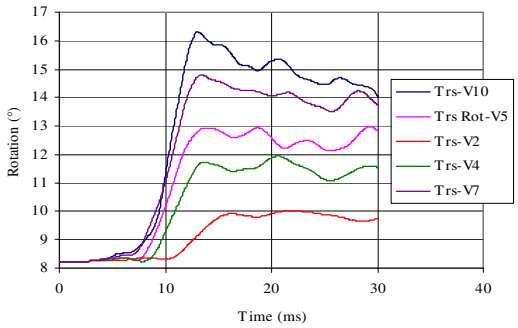

Figure 18. Knee torsion in the bending test.

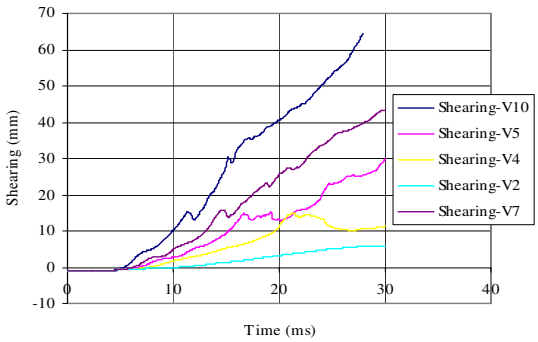

Figure 19. Knee lateral shearing in the shearing test.

In shearing tests, the two main kinematics aspects are the lateral shearing and the knee torsion (Figure 19). The lateral shearing seems to be correlated with velocity and rapidly reaches high values which are not relevant with geometrical characteristics of the proximal tibia and distal femur. At 15mm of shearing the curves reach a steady state which could result from the contact between intercondylar notch and tibia eminence. In the first 15 ms, the knee torsion reaches amplitudes ranging from 2° to 10° depending on the impact velocity (Figure 20).

For both impact situation rotation effects have to be linked to the asymmetrical geometry of the femoral condyle and the tibial glena. From a medical point of view, this torsion effect is described as a natural safety countermeasure of the human body during trauma situations in order to avoid (or limit) damage to ligaments.

The strain level recorded on each ligament (cruciate and lateral) and correlated to rotation or shearing effects were computed in total strain curve on the whole ligament and the maximum strain curve of local maximum strain level (Arnoux 2004). In this model analysis, the maximum strain can be considered as a first sensor to locate damage in the structure whereas the total strain gives a global overview of the whole structure. If the maximum strain reaches the ultimate strain level, we assume that damage can occur in the ligament. Moreover, if the ultimate strain level is reached on the total strain curve, the ligament complete failure can be postulated with a high probability.

For lateral bending tests, the lateral medial and the posterior cruciate ligaments were highly loaded and strain versus lateral bending seems to be independent of impact velocity (Figure 20). A small difference between maximum strain level and total strain level seems to show that the medial collateral ligament in the model has homogeneous strain distribution. Its maximum strain or total strain level used to postulate on damage in the ligaments is obtained with a lateral rotation ranging from 20 ° to 24 °. For the posterior cruciate ligament, the difference between global strain (maximum strain) and local strain (maximum strain) seems to confirmed local high strain levels. They were obtained on ligaments insertion and illustrated with Von Mises curve processing. Local damage could occur for knee rotation between 12 ° and 15 °, whereas global damage for knee lateral rotations was close to 26 ° (which seems to be very high).

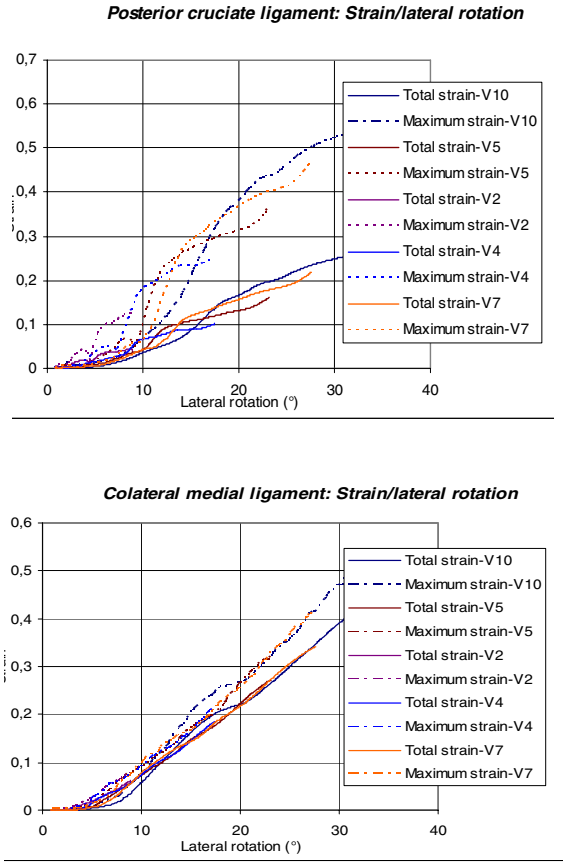

Figure 20. Posterior cruciate ligament total and maximum strain curves versus lateral rotation. Collateral medial ligament total and maximum strain curves versus lateral rotation.

For the shearing tests, the two cruciate and the tibial collateral ligaments were highly loaded (Figure 21). In that situation, impact velocity had no effects on strain versus knee shearing curves. The failure or damage could start at a 13 to 15 mm knee shearing. For the posterior cruciate ligament, the strain being not homogeneous on the structure, only maximum strain levels were computed, and they show that damage could occur for shear values ranging from 12 to 14 mm. Finally, for the collateral tibial ligament, the maximum strain reaches up to 14-17mm according to the impact velocity.

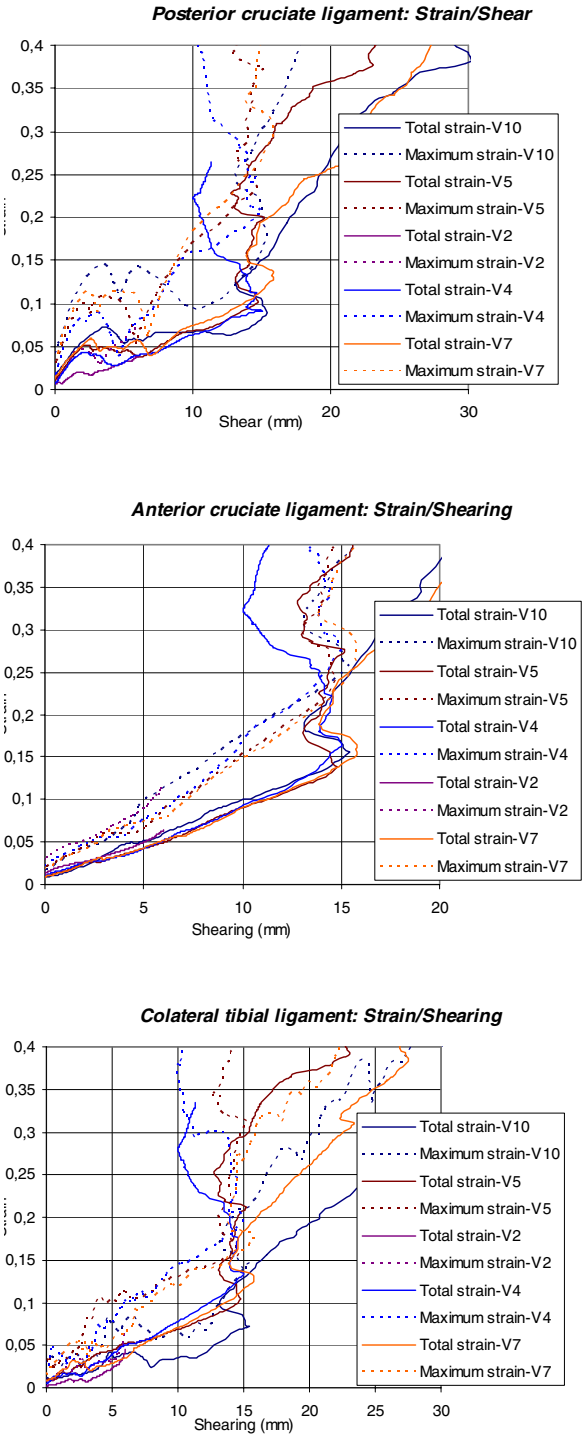

Figure 21. Total and maximum strain curves versus lateral shearing for the posterior cruciate ligament, the anterior cruciate ligament and the collateral tibial ligament.

DISCUSSION -CONCLUSION

Four test series were presented with the objective to evaluate the response of the lower limb to bending or shearing force. Impact tests were performed on isolated lower extremities of Post Mortem Human Subjects and biomechanical corridors have been proposed.

In bending tests, the differences between lower reaction force corridors for both impact velocities were only in magnitude, the rise time and the duration were equivalent. The first lower reaction force peak appears between 20 and 23 ms corresponding to a knee lateral flexion angle of 15-16°. Damage to the MCL was the most common joint damage induced in this test configuration; this is agreement with real word pedestrian accident injuries (Bhalla, 2003). Two fractures of the tibial plateau were noted for a 5.5m/s impact velocity (MFG10-MFG13). These damages could be induced by a greater valgus rotation of the knee at this speed causing a compression force on the tibial plateau. A vertical rotation of the lower limb was noted in all tests and is due to the no symmetric of the knee joint. The influence of this movement on the global response of the knee joint and the type/time of injury is unknown but may induce tensional forces in the knee joint ligaments.

In shearing experimental test, the upper impact load induced firstly bone injuries located near impact point as fracture of fibula head, lateral tibial condyles fractures or diaphysis fracture. These injuries could be tied to the first peak force, corresponding to a mean level of 1700N for an impact velocity of 4.2m/s and 2400N for an impact velocity of 5.5m/s. The following peaks are related to intra articular injuries as avulsion or rupture of the anterior cruciate ligament, and femoral cartilage injury. Note that tibial intercondylar eminence fractures were typical due to the shear force through the knee joint. In our tests, they were always associated with ACL damage.

Coupling such results with model analysis which allowed to record data unavailable experimentally and then to follow their evolution during the test, it was possible to complete injury mechanisms description and make correlation between peak in force and failure level reach on ligaments.

For the bending tests, the knee injury mechanism consisted in a lateral rotation around the contact area between the lateral femoral condyle the and tibial glena. This rotation simultaneously induces a high deflection of both anterior cruciate and medial collateral ligaments, assumed to be injured for rotations over 15 and 20 °respectively. These results were not sensitive to impact velocities, and seem to be relevant with those identified experimentally. Consequently, a conservative value of 15° for lateral rotation can be considered as ligaments injury criteria. For pure shearing impacts, the anterior, posterior cruciate

and tibial collateral ligaments were concerned. The ultimate shearing level was computed by recording the distance between the tibial eminence and the condylar notch that reached up to 13 to 15 mm whatever the impact velocity. Consequently, a conservative value of 13mm for shearing rotation can be considered as ligaments injury criteria.

The criteria postulated above were strongly dependant on the material properties. Model improvement with tissues a damage model as well as a parametric study around the failure criteria should be performed in order not to summarize the injury criteria to a single couple of value (lateral rotation and shearing) but also to define injury risk curves.

The strain versus time curves show the influence of impact velocity and the time dependent answer of the whole structure which could be mainly attributed to structure effects and also soft tissue viscoelastic properties. It also underlines the differences in strain distribution between cruciate and collateral ligaments. For the cruciate ligaments, high strain levels were recorded on ligaments insertions (in agreement with experimental results), that underlines failure properties of cruciate ligaments at their insertions.

Von Mises distribution was systematically located on the same metaphysis areas of the lower femur and upper tibia but also in the knee joint with contact area during shocks. This distribution could indicate a bending effect on the two bones. It was also observed that for impact velocities overs 10m/s, and according to the damping properties of the impacting surface, the failure risk for bones seems to be very high. Therefore, with numerical simulations, it was observed that even in pure loading, pure shearing or pure bending can not be obtained alone. The two mechanisms seem to be coupled with a majority of shearing or bending according to the loading conditions.

In perspective, new tests will be performed on suitably instrumented PMHS with objective to compare the effects of varying proportions of moment and shear applied at the knee joint. Further numerical simulations will be done in order to widen model capabilities by focussing on material properties and to improve injury criteria accuracy. The new experimental tests will be included in model validation process.

ACKNOWLEDGEMENT
We would like to thank MECALOG for their partnership in LLMS model designing.

REFERENCES

Aekbote K., Schuster P., Kankanala S., Sundararajan S., Rouhana W. 2003. “The biomechanical aspects of pedestrian protection“. Int. J. Vehicle Design, Vol. 32. 28-52

Arnoux P.J. 2000. « Modélisation des ligaments des membres porteurs », Ph D. Thesis.

Arnoux P.J., Kang H.S., Kayvantash K., Brunet C., Cavallero C., Beillas P., Yang H. 2001. “The Radioss Lower Limb Model for safety: application to lateral impacts”, International Radioss user Conference. Sophia

Arnoux P.J., Kang H. S., Kayvantash K. 2001. “The Radioss Human model for Safety”, Archives of Physiology and Biochemistry, vol. 109, 109.

Arnoux P.J., Cavallero C., Chabrand P., Brunet C. 2002. “Knee ligaments failure under dynamic loadings”. International Journal of Crashworthiness, Vol 7 (3), 255 – 268.

Arnoux P. J., Thollon L., Kayvantash K., Behr M., Cavallero C., Brunet C. 2002. “Advanced lower limb model with Radioss, application to frontal and lateral impact Radios lower limb model for safety”. Proceedings of the IRCOBI Conference.

Arnoux P. J., Cesari D., Behr M., Thollon L., Brunet C. 2004. “Pedestrian lower limb injury criteria evaluation a finite element approach”, under submission to Traffic Injury Prevention Journal.

Atkinson P., A stress based damage criterion to predict articular joint injury from subfracture insult, Ph.D. thesis, 1998.

Atkinson P.J., Haut R., Eusebi C., Maripudi V., Hill T., Sambatur K. 1998. “Development of injury criteria for human surrogates to address current trends in knee-to-instrument panel injury”, Stapp Car Crash Conference Proceedings. 13-28.

Beaugonin M., Haug E., Cesari D. 1996. “A numerical model of the human ankle/foot under impact loading in inversion and eversion”, 40th Stapp Car Crash Conference Proceedings.

Beaugonin M., Haug E., Cesari D. 1997. “Improvement of numerical ankle/foot model: modeling of deformable bone”, 41th Stapp Car Crash Conference Proc.

Bedewi P.G., Bedewi N.E. 1996. “Modelling of occupant biomechanics with emphasis on the analysis of lower extremities injuries”. International Journal of Crash, Vol. (1). 50-72.

Behr M., Arnoux P. J., Serre T., Bidal S., Kang H.S., Thollon L., Cavallero C., Kayvantash K., Brunet C. 2003. “A Human model for Road Safety : From geometrical acquisition to Model Validation with Radioss”, International Journal on Computer Methods in Biomechanics and Biomedical Engineering, vol 6 issue 4.

Behr M., Arnoux P.J., Thollon L., Serre T., Cavallero C., Brunet C. 2003. “Towards integration of muscle tone in lower limbs subjectes to impacts”, IX International Symposium on Computer Simulation in Biomechanics, Sydney, Australia.

Behr, M., Arnoux, P.J., Serre, T., Kayvantash, K., Brunet, C. 2005. “Modeling active muscle behavior for emergency braking simulations”. Computational Fluid and Solid Mechanics , Ed. Bathe. 60-64.

Beillas P., Modélisation des membres inférieurs en situation de choc automobile, Ph.D. thesis, École Nationale Supérieure d'Arts et Métiers, Paris, France, 1999

Beillas P., Lavaste F., Nicoloupoulos D., Kayventash K., Yang K. H., Robin S. 1999. “Foot and ankle finite element modeling using CT-scan data”, Stapp Car Crash Conference Proc.

Beillas P., Arnoux P. J., Brunet C., Begeman P., Cavallero C., Yang K., King A., Kang H. S., Kayvantash K., Prasad P. 2001. “Lower Limb: Advanced FE Model and New Experimental Data”, International Journal of STAPP - ASME, vol. 45, 469-493.

Bhalla K., Bose D., Madeley N.J., Kerrigan J., Crandall J., Longhitano D., Takahashi Y. 2003. “Evaluation of the Response of Mechanical Pedestrian Knee Joint Impactors in Bending and Shear Loading”. *18th International Conference on the Enhanced Safety of Vehicles.*

Bose D., Bhalla K., Rooij L., Millington S., Studley A., Crandall J. 2004. “Response of the Knee joint to the pedestrian impact loading environment”, SAE World Congress, paper 2004-01-1608.

Chawla A., Mukherjee S., Mohan D., Parihar A.. 2004. “Validation of Lower Extremity Model in THUMS”. IRCOBI Conf. 155-166

Eppinger R, Marcus J., Morgan R. 1984. ‘Develpment of Dummy and injury index for NHTSA’s Thoracic side impact protection research program’, SAE 840885, 28th Stapp Car Crash Conference, Warrendale, PA.

Grzegorz Teresinski, Roman Madro. 2001. “Pelvis and hip injuries as a reconstructive factors in car-to-pedestrian accidents”, Forensic Science International 124. 68-73.

Haut R. C., Atkinson P. J. 1995. “Insult to the human cadaver patellofemoral joint : effect of age on fracture tolerence and occult injury”, 39th Stapp Car Crash Conference Proc., SAE. 952729.

Hayashi S., Choi H.Y., Levine R.S., Yang K.H., King A.I. 1996. “Experimental and analytical study of knee fracture mechanisms in a frontal knee impact”, 40th Stapp Car Crash Conf. Proc.161.

IHRA/PS/200. 2001. International Harmonized Research Activities, Pedestrian Safety Working Group Report.

Ivarsson J, Lessley D, Kerrigan J, Bhalla K, Bose D., Crandall J, Kent R. 2004. ”Dynamic Response Corridors and Injury Thresholds of the Pedestrian Lower Extremities. IRCOBI Conference on the Biomechanics of Impacts.

Ivarsson J, Kerrigan J, Lessley D, Drinkwater C, Kam C, Murphy D, Crandall J, Kent R. 2005. “Dynamic “Response Corridors of the Human Thigh and Leg in Non-Midpoint Three-Point Bending.” Society of Automotive Engineers World Congress. Paper Number 05B-218.

Kajzer J., Cavallero C., Bonnoit J., Morjane A., Ghanouchi S. 1990. “Response of the knee joint in lateral impact: Effect of shearing loads”. Proc. IRCOBI. 293-304.

Kajzer J., Cavallero C., Bonnoit J., Morjane A., Ghanouchi S. 1993. “Response of the knee joint in lateral impact: Effect of bending moment.” Proc. IRCOBI. 105-116.

Kallina I, 2002. “Pedestrian Protection. Looking for Potentials”. Proc. IRCOBI. 1–15.

Kerrigan J.R., Ivarsson B.J., Bose D., Madeley N.J., Millington S.A., Bhalla K. S., Crandall J.R. 2003. “Rate sensitive constitutive and failure properties of human collateral knee ligaments”, IRCOBI conference. 193

Maltese M.R., Eppinger R. H., Rhule H., Donnelly B., Pintar F. A., Yoganandan N. 2002. “Response Corridors of Human Surrogates in lateral impacts”. Stapp Car Crash Journal, vol. 46.

Schuster P.J., Chou C.C., Prasad P., Jayaraman G. 2000. “Development and Validation of a Pedestrian Lower Limb Non-Linear 3-D Finite Element

Model". 44th Stapp Car Crash Conference Proceedings. Atlanta, 2000-01-SC21.

Stutts J.C., Hunter, W.W. 1999. "Motor vehicle and roadway factors in pedestrian and bicyclists injuries: an examination based on emergency department data", Accident analysis and prevention. Volume 31, Issue 5, Pages 505-514.

Subit D.2004. "Modélisation de la liaison os ligament dans l'articulation du genou", PhD. Thesis, Université de la Méditerranée.

Subit D., Chabrand P., Masson C., Brunet C. 2004. "Modelling of the mechanical behaviour of the insertion of the ligament to bone in knee joint." Congress of European Society of Biomechanics, s'-Hertogenbosch.

Subit D., Chabrand P., Masson C., Brunet C. 2004 "Behaviour of human knee ligaments : tensile tests in flexion and extension." 12th International Conference On Experimental Mechanics. Bari.

Takahashi Y., Kikuchi, Y., Mori, F., and Konosu, A., 2003 "Advanced FE Lower Limb Model for Pedestrians". 18th International Conference on the Enhanced Safety of Vehicles.

Tannous R.E., Bandak F.A., Toridis T.G., Eppinger R.H. 1996. "A three-dimensional finite element model of the human ankle: development and preliminary application to axial impulsive loading", 40th Stapp Car Crash Conference Proc., SAE. 219-238.

Winkler G. 1974. Manuel d'Anatomie Topographique et Fonctionnelle, 2nd ed. Masson, Paris.

Yang J. 1997. "Injury Biomechanics in car pedestrian collisions: development, validation and application of Human-Body mathematical models". Ph.D. thesis.